Design of an on-chip microscale nanoassembly system

Jason J. Gorman,* Yong-Sik Kim,
András E. Vladár and Nicholas G. Dagalakis

Manufacturing Engineering Laboratory,
National Institute of Standards and Technology,
Gaithersburg, MD 20899 USA
E-mail: gorman@nist.gov
E-mail: yongsik.kim@nist.gov
E-mail: andras.vladar@nist.gov
E-mail: dagalakis@nist.gov
*Corresponding author

Abstract: A microscale nanoassembly system has been designed for the fabrication of nanodevices and *in situ* electromechanical characterisation of nanostructures. This system consists of four Microelectromechanical Systems (MEMS)-based nanomanipulators positioned around a centrally located port for introducing nanostructure samples. Each nanomanipulator is composed of an *XYZ* nanopositioning mechanism with an attached nanoprobe for interacting with the nanostructures. By simultaneously controlling the position of each of these nanoprobes, they can be used to cooperatively assemble complex structures. The static and dynamic motion characteristics of a prototype nanomanipulator have been measured, providing a non-linear calibration of the quasi-static input–output behaviour, as well as values for the system bandwidth and structural natural frequencies. Important operational issues including proposed manipulation schemes, precision motion control and integration with a Scanning Electron Microscope/Focused Ion Beam (SEM/FIB) instrument are also discussed.

Keywords: nanoassembly; probe-based nanomanipulation; nanomanipulator; microelectromechanical systems; MEMS.

Reference to this paper should be made as follows: Gorman, J.J., Kim, Y-S., Vladár, A.E. and Dagalakis, N.G. (2007) 'Design of an on-chip microscale nanoassembly system', *Int. J. Nanomanufacturing*, Vol. 1, No. 6, pp.710–721.

1 Introduction

This paper discusses the design and characterisation of a novel microscale nanoassembly system intended for the fabrication and *in situ* electromechanical characterisation of nanodevices. Existing macroscale nanomanufacturing tools for nanoassembly, such as Atomic Force Microscopes (AFM) and nanomanipulators, have limited manipulation capabilities, and their large size and high cost prohibit their use in many applications. The utilisation of Microelectromechanical Systems (MEMS) for the development of fully

Copyright © 2007 Inderscience Enterprises Ltd.

integrated nanomanufacturing workcells on a single silicon chip has a number of advantages over existing macroscale systems. The reduction in size simplifies integration with other instruments such as Scanning Electron Microscopes (SEM), reduces the effects of thermal drift by reducing the amount of material used, and allows the manufacturing and measurement accuracy to be significantly improved due to the close proximity between the workpiece and system sensors and actuators. Batch fabrication of nanomanufacturing systems will dramatically reduce startup costs, and also enable massively parallel tools for high-throughput manufacturing. Furthermore, retooling these systems only requires redesign and fabrication at a minimal cost compared to overhauling macroscale equipment.

The utilisation of MEMS for nanotechnology research has recently received attention by a number of researchers. MEMS nanopositioning mechanisms for ultra-precision motion applications have been developed by Bergna et al. (2005), Chen and Culpepper (2006). Other microscale instruments that have been demonstrated include a microscale AFM (Xu et al., 1995) and an atomic trapping and cooling apparatus (Gollasch et al., 2005). In all of these examples, the main challenge in scaling down the dimensions of an instrument is maintaining the same level of operational precision as the equivalent macroscale instrument. Limits in microfabrication processes, viable materials and tolerances make this challenge difficult. In particular, tolerances in standard photolithography for MEMS can result in significant geometric uncertainties for devices with critical dimensions on the order of a few micrometers. Therefore, it is important that the benefits of reduced size and cost, among others, are weighed against the difficulties in achieving nanoscale precision with microscale mechanisms.

The synthesis of nanostructures with unique physical properties, such as nanowires and nanoparticles, presents many opportunities for novel nanoelectromechanical systems, and has become one of the cornerstones of nanotechnology research. However, accurate and repeatable methods for manipulating these nanostructures and assembling them into functional nanodevices are not currently available. Manipulation and assembly at the nanoscale is a particularly difficult problem that has so far received only limited attention. Carbon nanotubes have been successfully manipulated using an AFM for structural experiments by Yu et al. (1999). The mechanical interactions between an AFM tip and nanoparticles during manipulation on a substrate have been modelled and utilised to improve manipulation by Sitti and Hashimoto (2000). This manipulation approach has also been extended to include the assembly of polymer nanoparticles and their subsequent thermal bonding (Harel et al., 2005). Although AFMs are capable of nanomanipulation and are an obvious choice due to their widespread availability, they have many limitations as a nanomanipulator. Most importantly, they are generally limited to a single probe with 3 Degrees of Freedom (DOF). Furthermore, the AFM cantilever occludes the manipulation manoeuvre, making it difficult to utilise visual feedback from an SEM.

A similar but improved approach to AFM nanomanipulation is the use of a sharp tipped nanoprobe that can be positioned with nanometer resolution, as has been demonstrated for micromanipulation by Kasaya et al. (2004). In this case, the manipulation of nanostructures can be visualised with an SEM without occlusion while the basic approach of AFM nanomanipulation, pushing with the tip of a sharp probe, is maintained. In this paper, the design and proposed operation of a MEMS-based nanoassembly system designed for probe-based nanomanipulation are presented. The nanoassembly system is comprised of four nanomanipulators that can work

independently or cooperatively to assemble nanodevices. The design of the nanomanipulators will be discussed and experimental motion characterisation results for one nanomanipulator will be presented. Three important operational issues for this system are then discussed: nanomanipulation strategies using the nanoassembly system, MEMS precision motion control and integration of the on-chip nanoassembly system with an SEM/FIB instrument to obtain a complete nanomanufacturing environment.

2 System design

The objective of the design for the microscale nanoassembly system is to create a tool for nanoscale manipulation and assembly using probe-based techniques which can operate inside an SEM. A schematic of the system design is shown in Figure 1. The system is composed of four nanomanipulators that are arranged in a 2 × 2 array on a silicon chip. Each nanomanipulator consists of an *XYZ* MEMS nanopositioner with a single nanoprobe attached. The four nanomanipulators share a common workspace around the sample port at the centre of the array, as shown in Figure 2. The sample port is an opening in the silicon chip through which a sample substrate containing nanostructures can be positioned. By coordinating the motion of all four nanomanipulators, complex nanoassembly functionalities can be achieved. Parallel nanoassembly is possible by increasing the number of nanomanipulators in the array.

Figure 1 Microscale nanoassembly cell with 2 × 2 array of *XYZ* nanomanipulators

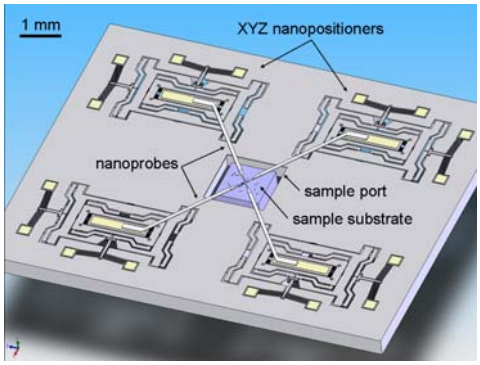

Figure 2 Multiple nanoprobes working in a shared workspace

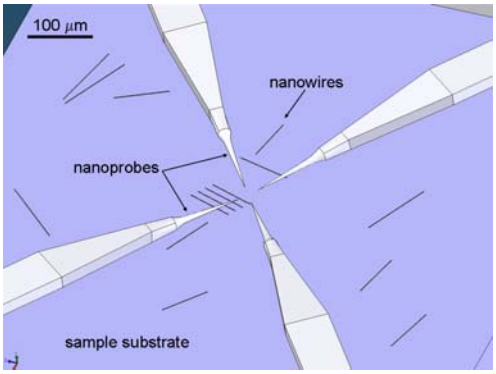

As a first step in this project, we have designed and fabricated a 2 × 2 array of *XYZ* MEMS nanopositioners based on the nanopositioning mechanisms presented in Bergna et al. (2005). One of these prototypes is shown in Figure 3. The *X* and *Y* axes are actuated by bent-beam thermal actuators, which were chosen due to their high stiffness and large output force. These actuators apply forces along their respective axes to the flexure mechanism, resulting in planar displacement of the centre stage. The flexure mechanism design utilises a parallel dual-lever to amplify the motion along the axis of desired motion while minimising crosstalk between the *X* and *Y* axes. Motion along the *Z* axis is generated by applying a force perpendicular to the centre stage, which is supported by four serpentine springs. An electromagnetic actuator prototype has been designed for driving this DOF. The actuator is composed of a microcoil located on a second chip, and a moving platform similar to the centre stage shown in Figure 3. Permalloy (80% Ni–20% Fe) is deposited on the back side of the moving platform, and the two chips are bonded together. Applying a current to the microcoil generates a magnetic field, which in turn causes a magnetic force on the moving platform. We are currently working on integrating this actuator scheme into the nanoassembly system.

Figure 3 Fabricated microscale *XYZ* nanomanipulator

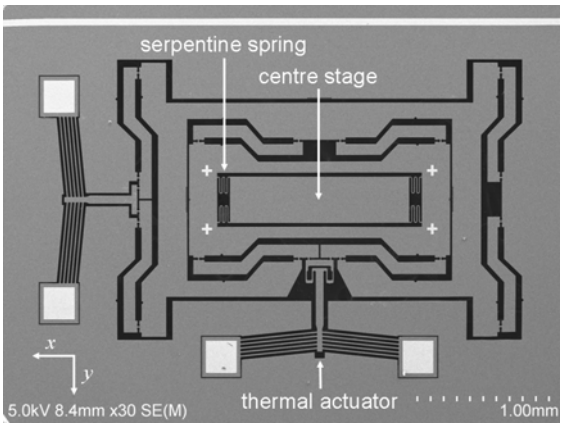

3 Mechanism characterisation

The *XYZ* nanopositioner shown in Figure 3 is a critical element in the nanoassembly system and must perform manipulation manoeuvres with nanoscale precision. In this section, we discuss some initial experimental characterisation results for this mechanism. Firstly, results for the static calibration of the relationship between the input voltage and resulting displacement of the mechanism are discussed. Then, results on the crosstalk between the *X* and *Y* axes are presented. Finally, measurements of system frequency responses are discussed.

The quasi-static relationship between the mechanism displacement and input voltage was measured using an optical microscope with a digital camera. The input voltage was varied and at each input voltage an image was captured at 100 times magnification. Applying image processing to the sequence of images for the *X* and *Y* axes results in the data shown in Figures 4 and 5. In general, the behaviour of the mechanism is as expected, where the displacement is a quadratic function of the input voltage. This is due

to the fact that the temperature of the actuator is a function of the power dissipation caused by Joule heating. It was found that for a voltage range of 0–10 V the displacement was 5.0 μm along the *X*-axis and 3.4 μm along the *Y*-axis. These values are significantly smaller than those found for a 1 DOF mechanism of similar dimensions (Bergna et al., 2005). This is likely due to a change in stiffness of the flexure mechanism due to coupling between the *X* and *Y* axes. Additionally, the data shows that the mechanism strays from the quadratic behaviour at 10 V for both axes, indicating that there may be some electrical coupling in the mechanism that is causing the reduced displacement. Optimisation of the flexure mechanism for increased range will be explored in the future and we are currently investigating methods for electrically isolating individual axes.

Figure 4 Displacement versus input voltage for *X*-axis

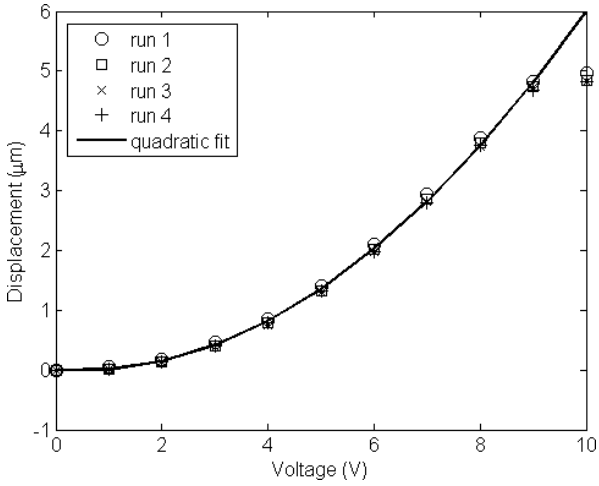

Figure 5 Displacement versus input voltage for *Y*-axis

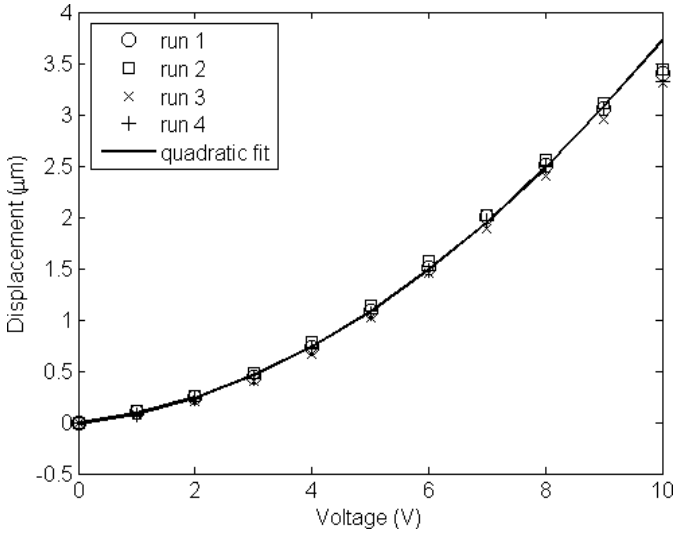

As mentioned previously, the *X* and *Y* axes are mechanically coupled through the flexure mechanism. Therefore, coupled motion is expected, otherwise known as crosstalk. The crosstalk between these axes was measured by actuating one axis while measuring the displacement of the orthogonal axis using the method described above. The crosstalk as a function of input voltage in the *X* and *Y* axes for a voltage range of 0–10 V is shown in Figures 6 and 7. The maximum crosstalk was found to be approximately 220 and 250 nm in the *X* and *Y* directions, respectively. Additionally, the data shows that the crosstalk follows a quadratic curve that is not centred about the origin. Comparing this result to the displacement data in Figures 4 and 5, the percentage crosstalk for full range displacement is 6.1%. Although this result is not optimal, this level of coupling could be compensated and the effect on the manipulation precision would likely not be a significant problem.

Figure 6 Crosstalk along *Y*-axis when input voltage is applied to *X*-axis

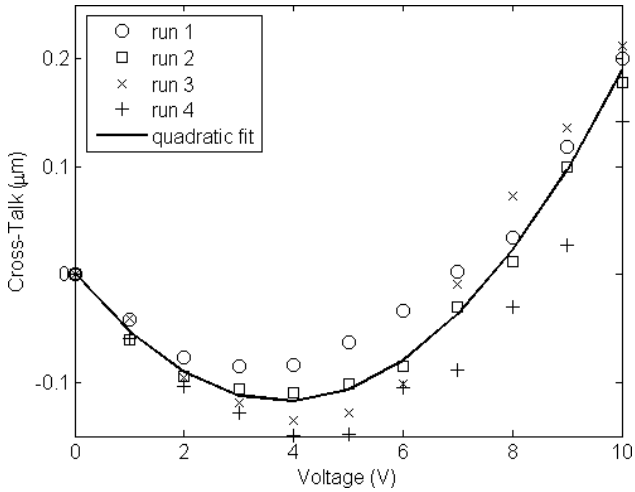

Figure 7 Crosstalk along *X*-axis when input voltage is applied to *Y*-axis

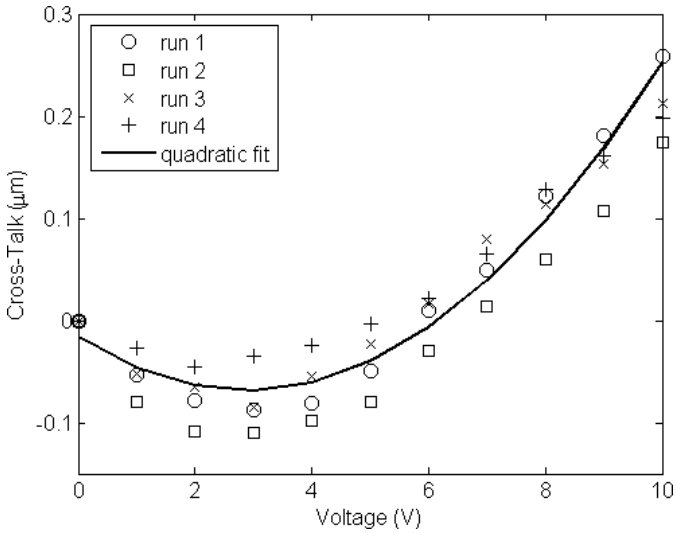

Finally, the frequency response of the mechanism was measured to determine the actuator bandwidth and the effects of resonance on the mechanism's motion. The frequency responses were measured using the swept-sine method and a laser reflectance microscope which provides an in-plane measurement of the motion of the mechanism, as discussed in Gorman et al. (2006). Since the thermal actuator response is non-linear, the measurements were performed with a 5 V bias on the input voltage and a small excitation signal (≈ 500 mV peak-to-peak). Both the actuator and mechanism responses were measured for the *X* and *Y*-axes. Figure 8 shows the frequency response of the thermal actuator and the entire mechanism for the *X*-axis. Since the flexure mechanism amplifies the motion of the actuator, the motion of the flexure mechanism is larger than the thermal actuator. However, for the purpose of comparison, the frequency responses have been normalised. This data clearly shows that the system dynamics are a combination of a first-order response due to the thermal actuator, and the structural modes of the flexure mechanism. In general, the response for the actuator is similar to the overall mechanism. The working bandwidth for the *X*-axis was determined to be approximately 65 Hz and the first structural natural frequency is 9.355 kHz.

Figure 8 Experimental frequency response for *X*-axis

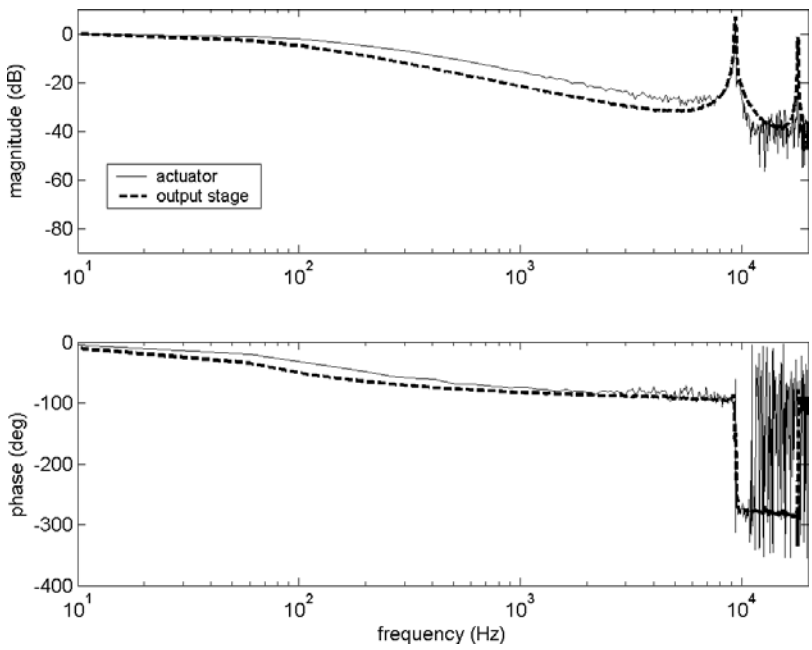

The frequency responses along the *Y*-axis demonstrate a fundamental difference, as shown in Figure 9. Here the response of the actuator is free of any resonances, while the measurement for the entire mechanism is shown to have a resonance. This is most likely due to the fact that the *Y*-axis is designed to be decoupled from the *X*-axis when the *X*-axis displacement is zero. However, the *X*-axis is not decoupled from the *Y*-axis, even when the *Y*-axis displacement is zero. This coupling can be seen in Figure 3, where the *Y*-axis actuator clearly causes a moment on the flexure mechanism when the *X*-axis displaces. The working bandwidth for the *Y*-axis was determined to be approximately 42 Hz and the first structural natural frequency is 6.576 kHz.

Figure 9 Experimental frequency response for *Y*-axis

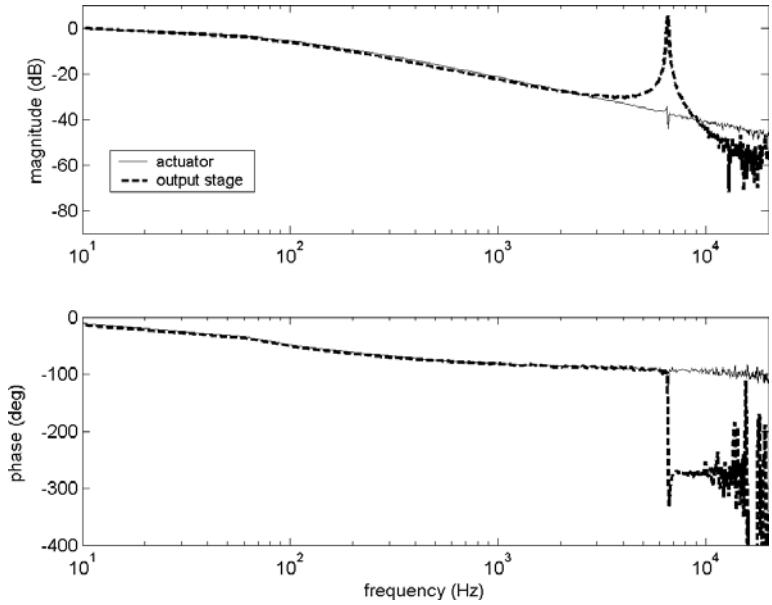

The dynamic response of the mechanism is critical to its performance in nanomanipulation because it determines the fastest rate at which the nanomanipulator can move without vibration. Finite element analysis was applied to the design to determine the expected first modes of vibration for the *X* and *Y* directions. The first natural frequencies along the *X* and *Y* axes were found to be 9.962 and 7.586 kHz, respectively, resulting in a percent error of 6.4% and 18.4%. These discrepancies are reasonable due to the anisotropic nature of silicon and the uncertainty in Young's modulus for variations in doping levels. Similar to the results in Gorman et al. (2006), in the future we will apply a non-linear model to this data and then design a closed-loop controller that will maximise the bandwidth while maintaining nanoscale position resolution.

4 Important research topics

The design of the on-chip nanoassembly system is only the first step in implementing a precision nanoassembly environment. In addition to our research on the proposed mechanism, a number of problems must be solved including the development of repeatable manipulation manoeuvres using multiple nanoprobes, precision motion control and the integration of the nanoassembly system within an SEM/FIB instrument. Some of our plans for addressing these problems are discussed in the following subsections.

4.1 Manipulation strategies

Manipulating nanoscale structures is particularly challenging since surface forces, including van der Waals, electrostatic and capillary forces, dominate the dynamics at

this scale. In general, the motion of a nanostructure when pushed along a surface is not deterministic because surface forces are inhomogeneous due to variations in surface roughness, charge and water adsorption. Therefore, successful manipulation schemes must be developed which constrain the manipulated nanostructure for deterministic motion in an inhomogeneous force field while also minimising the contact area between the nanostructure and manipulation tools. We intend to address this problem by designing specific manipulation primitives and developing simulation models for verifying the manipulation strategies offline.

Implementing manipulation schemes with nanoprobes as manipulation tools minimises the contact area between the tool and nanostructure, and provides a number of useful and interesting functionalities. Using a single nanoprobe, a nanostructure might be pushed on a surface for planar assembly, and under the proper environmental conditions could be manipulated in three dimensions by utilising adhesion (Figure 10(a)). As mentioned previously, using only a single nanoprobe is difficult due to inhomogeneous surface forces, but the approach works in some situations.

Figure 10 Nanomanipulation of a nanowire using nanoprobes. (a) Manipulation via adhesion, (b) manipulation via gripping, (c) rotating a nanowire with two nanoprobes and (d) assembly using v-notch fixtures

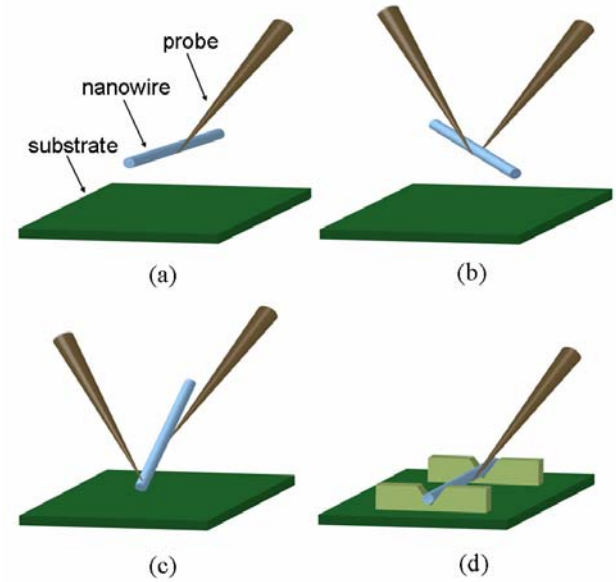

Multiple nanoprobe manipulation strategies are needed to properly constrain a nanostructure during assembly. Two nanoprobes could be used as tweezers for grabbing a single nanostructure (Figure 10(b)). They could also be used for three dimensional operations such as rotating a nanostructure (Figure 10(c)). This could be extended to three nanoprobes, where two are used to grip the nanostructure while the third is used to rotate the nanostructure about its gripping point. Since adhesion can hinder the release of nanostructures when assembling a device, simple and repeatable methods for accurate placement are needed. The most straightforward approach is to use nanofabricated fixtures such as v-notches (Figure 10(d)). Here, the adhesion forces are dominated by the contact forces, likely yielding a repeatable release.

4.2 Precision motion control

Precision motion control of these mechanisms is critical for successful nanoassembly. An open-loop control approach has been developed to achieve motion resolution on the order of tens of nanometers by calibrating the input (voltage)–output (displacement) relationship of the mechanism and then inverting this relationship to calculate the required control voltage for a desired motion profile. As an example of the motion resolution that can be achieved using this approach, a prototype nanomanipulator was controlled to perform 50 nm steps, as shown in Figure 11. The motion was measured in an SEM and the resolution was found to be smaller than +/– 7 nm. Although this level of control would be acceptable for some applications, the open-loop approach has been found to only be repeatable within a small range (+/– 1 μm), and errors become unacceptable for larger excursions.

Closed-loop control is currently being explored to achieve nanoscale precision over the entire range and to improve the dynamic response. Firstly, position sensors must be included in the mechanism design. Although capacitive sensors typically have the best resolution and stability, a comb structure with the required capacitance is likely to be larger than would be acceptable for the nanoassembly array. Therefore, we are also currently working on the design of piezoresistive position sensors. With the addition of feedback, the non-linear PID controller discussed in Gorman et al. (2006) will then be implemented.

Figure 11 Open-loop nanopositioning of a prototype nanomanipulator (50 nm steps)

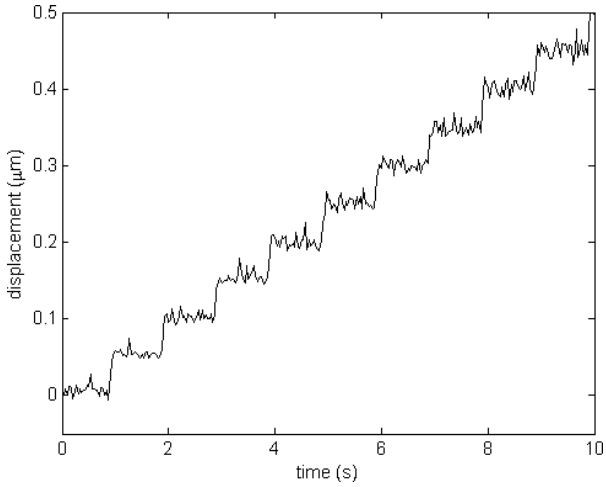

4.3 SEM/FIB integration

Upon completion of the nanoassembly system, the necessary integration for operation within an SEM/FIB will be performed. The long-term goal of this project is to combine nanoassembly, nanoscale imaging, and FIB material deposition and milling into a complex and capable nanomanufacturing system. Although FIB deposition and milling are now common approaches in nanotechnology research (Reyntjens and Puers, 2001), there are still many issues to be resolved in their use with levels of precision and

repeatability expected of a nanomanufacturing system. Additionally, the interactions between the nanoassembly system and the SEM/FIB system will present many new challenges.

One prototype assembly operation that highlights many of the processes that will be handled by this nanomanufacturing system is the assembly of a nanowire resonator. A nanowire is first manipulated to isolate it from other structures. The FIB is then used to cut the nanowire to the proper size. Then, the nanowire is placed across two electrical contacts using the nanoassembly system. Platinum is then deposited over the ends of the nanowire to bond it to the contacts using the FIB. Finally, the nanoassembly system can be used to probe the nanowire device for electrical and mechanical measurements. Within this process there are a number of issues that must be explored and solved for repeatable manufacturing. In particular, the interactions between the FIB and the nanoassembly system, such as contamination of the nanoprobes with precursor components, will be investigated. Furthermore, the mechanical and electrical quality of platinum deposition for nanowire bonding requires further investigation (Cronin et al., 2002; Nam et al., 2005).

5 Conclusion

This paper has discussed a design for an on-chip microscale nanoassembly system that is currently under development. A prototype nanomanipulator has been fabricated and its static and dynamic motion behaviour have been characterised. The mechanism appears to be suitable for nanoassembly and is being redesigned for increased motion range. Additional research objectives have also been outlined that are critical for the success of this project, including manipulation strategies, precision motion control and integrating the nanoassembly system with an SEM/FIB. If successful, this project will result in an on-chip nanomanufacturing system that would be the first of its kind.

References

Bergna, S., Gorman, J.J. and Dagalakis, N.G. (2005) 'Design and modeling of thermally-actuated MEMS nanopositioners', *Proceedings of the ASME IMECE*, Orlando, FL, IMECE2005-82158.

Chen, S-C. and Culpepper, M.L. (2006) 'Design of a six-axis micro-scale nanopositioner – μHexFlex', *Precision Engineering*, Vol. 30, pp.314–324.

Cronin, S.B., Lin, Y-M., Rabin, O., Black, M.R., Ying, J.Y., Dresselhaus, M.S., Gai, P.L., Minet, J-P. and Issi, J-P. (2002) 'Making electrical contacts to nanowires with a thick oxide coating', *Nanotechnology*, Vol. 13, pp.653–658.

Gollasch, C.O., Moktadir, Z., Kraft, M., Trupke, M., Eriksson, S. and Hinds, E.A. (2005) 'A three-dimensional electrostatic actuator with a locking mechanism for microcavities on atom chips', *Journal of Micromechanics and Microengineering*, Vol. 15, pp.S39–S46.

Gorman, J.J., Kim, Y-S. and Dagalakis, N.G. (2006) 'Control of MEMS nanopositioners with nano-scale resolution', *Proceedings of the ASME IMECE*, Chicago, IL, IMECE2006–16190.

Harel, E., Meltzer, S.E., Requicha, A.A.G., Thompson, M.E. and Koel, B.E. (2005) 'Fabrication of polystyrene latex nanostructures by nanomanipulation and thermal processing', *Nanoletters*, Vol. 5, pp.2624–2629.

Kasaya, T., Miyazaki, H.T., Saito, S., Koyano, K., Yamaura, T. and Sato, T. (2004) 'Image-based autonomous micromanipulation system for arrangement of spheres in a scanning electron microscope', *Review of Scientific Instruments*, Vol. 75, pp.2033–2042.

Nam, C.Y., Kim, J.Y. and Fischer, J.E. (2005) 'Focused-ion-beam platinum nanopatterning for GaN nanowires: ohmic contact and patterned growth', *Applied Physics Letters*, Vol. 86, 193112.

Reyntjens, S. and Puers, R. (2001) 'A review of focused ion beam applications in microsystems technology', *Journal of Micromechanics and Microengineering*, Vol. 11, pp.287–300.

Sitti, M. and Hashimoto, H. (2000) 'Controlled pushing of nanoparticles: modeling and experiments', *IEEE/ASME Transactions on Mechatronics*, Vol. 5, pp.199–211.

Xu, Y., MacDonald, N.C. and Miller, S.A. (1995) 'Integrated micro-scanning tunneling microscope', *Applied Physics Letters*, Vol. 67, pp.2305–2307.

Yu, M-Y., Dyer, M.J., Skidmore, G.D., Rohrs, H.W., Lu, X-K., Ausman, K.D., Von Her, J.R. and. Ruoff, R.S. (1999) 'Three-dimensional manipulation of carbon nanotubes under a scanning electron microscope', *Nanotechnology*, Vol. 10, pp.244–252.